CLOSED-FORM SOLUTIONS FOR AN EDGE DISLOCATION INTERACTING
WITH A PARABOLIC OR ELLIPTICAL ELASTIC INHOMOGENEITY
HAVING THE SAME SHEAR MODULUS AS THE MATRIX

Xu Wang and Peter Schiavone

msp

CLOSED-FORM SOLUTIONS FOR AN EDGE DISLOCATION INTERACTING WITH A PARABOLIC OR ELLIPTICAL ELASTIC INHOMOGENEITY HAVING THE SAME SHEAR MODULUS AS THE MATRIX

Xu Wang and Peter Schiavone

We use complex variable methods to derive closed-form solutions to the problems of an edge dislocation interacting with a parabolic or elliptical elastic inhomogeneity embedded inside an infinite elastic matrix. The inhomogeneity and the matrix have the same shear modulus but distinct Poisson's ratios. The edge dislocation can be located in the matrix, in the elastic inhomogeneity or precisely on the parabolic or elliptical interface. Explicit expressions of the image force acting on the edge dislocation as a result of its interaction with the parabolic or elliptical elastic inhomogeneity are presented. Our analyses indicate that the image force on an edge dislocation inside a parabolic or an elliptical elastic inhomogeneity is invariant with the direction of the Burgers vector of the edge dislocation.

1. Introduction

Green's functions for composites subjected to a line dislocation and/or a line force have been studied extensively by many investigators (see, for example, [Dundurs 1969; Stagni 1982; 1993; 1999; Warren 1983; Stagni and Lizzio 1983; Suo 1989; 1990; Tsuchida et al. 1991; Gong and Meguid 1994; Qaissaunee and Santare 1995; Yen et al. 1995; Ting 1996; Chen 1996; Wang and Sudak 2006; Wang 2015; Shi and Li 2006]). It appears that exact and closed-form representations of Green's functions exist only in cases involving two bonded isotropic or anisotropic elastic half-planes and for problems involving circular isotropic elastic inhomogeneities [Dundurs 1969; Ting 1996; Wang 2015]. Series-form representations of Green's functions are available for elliptical and nonelliptical elastic inhomogeneities [Stagni 1982; 1993; 1999; Warren 1983; Stagni and Lizzio 1983; Tsuchida et al. 1991; Gong and Meguid 1994; Qaissaunee and Santare 1995; Yen et al. 1995; Ting 1996; Chen 1996; Wang and Sudak 2006].

In this paper, we study the plane problems associated with an edge dislocation interacting with a parabolic or elliptical elastic inhomogeneity. The edge dislocation can be located in the matrix, in the elastic inhomogeneity or even on the parabolic or elliptical interface. Using Kolosov–Muskhelishvili's complex variable formulation [Muskhelishvili 1953], we demonstrate that elementary closed-form solutions can still be obtained when the elastic inhomogeneity and the matrix have equal shear moduli but distinct Poisson's ratios. Using the Peach–Koehler formula [Dundurs 1969], explicit expressions of the image force acting on the edge dislocation are presented. Some interesting features of the image force are observed, especially when the edge dislocation lies inside the elastic inhomogeneity. The paper is structured as follows. Kolosov–Muskhelishvili's complex variable formulation is briefly reviewed in Section 2. Closed-form solutions are derived in Section 3 for an edge dislocation interacting with a

parabolic elastic inhomogeneity. Closed-form solutions are derived in Section 4 for an edge dislocation interacting with an elliptical elastic inhomogeneity. In Section 5, we present a closed-form expression of the image force on an edge dislocation inside an elastic inhomogeneity of arbitrary shape having the same shear modulus as that of the matrix. In Section 6, we obtain a closed-from expression of the image force on an edge dislocation in an infinite matrix reinforced by an elastic inhomogeneity of arbitrary shape having the same shear modulus as that of the matrix. We summarize our findings and conclusions in Section 7. We remark that since an edge dislocation is a defect in a crystalline solid, its mobility and stability resulting from its interaction with an elastic inhomogeneity of parabolic, elliptical or nonelliptical shape is of fundamental importance in understanding the mechanical properties of the corresponding composite structure. In our case, this can be clearly observed from the obtained closed-form expressions for the image force acting on the edge dislocation.

2. Kolosov–Muskhelishvili's complex variable formulation

A Cartesian coordinate system $\{x_i\}$ $(i = 1, 2, 3)$ is established. For the in-plane deformations of an isotropic elastic material, the three in-plane stresses $(\sigma_{11}, \sigma_{22}, \sigma_{12})$, two in-plane displacements (u_1, u_2) and two stress functions (ϕ_1, ϕ_2) are given in terms of two analytic functions $\varphi(z)$ and $\psi(z)$ of the complex variable $z = x_1 + ix_2$ as [Muskhelishvili 1953]

$$
\begin{aligned}
\sigma_{11} + \sigma_{22} &= 2[\varphi'(z) + \overline{\varphi'(z)}], \\
\sigma_{22} - \sigma_{11} + 2i\sigma_{12} &= 2[\bar{z}\varphi''(z) + \psi'(z)],
\end{aligned}
\tag{1}
$$

$$
\begin{aligned}
2\mu(u_1 + iu_2) &= \kappa\varphi(z) - z\overline{\varphi'(z)} - \overline{\psi(z)}, \\
\phi_1 + i\phi_2 &= i[\varphi(z) + z\overline{\varphi'(z)} + \overline{\psi(z)}],
\end{aligned}
\tag{2}
$$

where $\kappa = 3 - 4\nu$ for plane strain and $\kappa = (3 - \nu)/(1 + \nu)$ for plane stress, μ and ν $(0 \leq \nu \leq 1/2)$ are the shear modulus and Poisson's ratio, respectively. In fact, energy considerations dictate that the range of Poisson's ratio can be relaxed to $-1 \leq \nu \leq 1/2$: materials with a negative Poisson's ratio are referred to as 'auxetic materials' [Lakes 1987; Argatov et al. 2012]. In addition, the in-plane stresses are related to the two stress functions through [Ting 1996]

$$
\sigma_{11} = -\phi_{1,2}, \quad \sigma_{12} = \phi_{1,1}, \quad \sigma_{21} = -\phi_{2,2}, \quad \sigma_{22} = \phi_{2,1}.
\tag{3}
$$

In fact, the stress expressions in (1) can be obtained after differentiation of the stress functions in $(2)_2$. Thus, Equation (2) is fundamental to the formulation.

3. An edge dislocation interacting with a parabolic elastic inhomogeneity

3.1. *Problem description.* As shown in Figure 1, a parabolic elastic inhomogeneity, denoted by S_1, is perfectly bonded to the surrounding matrix, denoted by S_2, through a parabolic interface L described by

$$
L : x_1 = H - \frac{x_2^2}{4H}, \quad H > 0.
\tag{4}
$$

In addition, an edge dislocation with Burgers vector (b_1, b_2) is located at $z = z_0 = x_0 + iy_0 = re^{i\theta}$ with x_0 and y_0 being the Cartesian coordinates of z_0 whilst r and θ represent the polar coordinates of z_0.
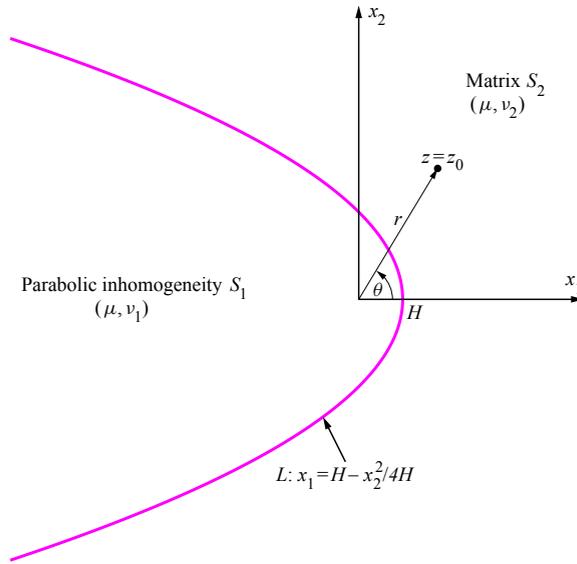
Figure 1. An edge dislocation interacting with a parabolic elastic inhomogeneity. The edge dislocation located at $z = z_0$ can be in the matrix, in the inhomogeneity or just on the parabolic interface.

Throughout the paper, subscript 1 and 2 are used to identify the respective quantities in S_1 and S_2 (we remark that this notation clearly does not apply to the two components of the Burgers vector.) In order to arrive at closed-form solutions, we assume that the parabolic inhomogeneity and the matrix have the same shear modulus but distinct Poisson's ratios (i.e., $\mu_1 = \mu_2 = \mu$ and $\nu_1 \neq \nu_2$).

It follows from (2) that the conditions representing continuity of tractions and displacements across the perfect parabolic interface L can be expressed in terms of the two pairs of analytic functions $\varphi_i(z)$, $\psi_i(z)$ ($i = 1, 2$) as follows:

$$\begin{aligned} \varphi_1(z) + z\overline{\varphi_1'(z)} + \overline{\psi_1(z)} &= \varphi_2(z) + z\overline{\varphi_2'(z)} + \overline{\psi_2(z)}, \\ \kappa_1\varphi_1(z) - z\overline{\varphi_1'(z)} - \overline{\psi_1(z)} &= \kappa_2\varphi_2(z) - z\overline{\varphi_2'(z)} - \overline{\psi_2(z)}, \quad z \in L. \end{aligned} \tag{5}$$

Equation (5) can be conveniently rewritten in the form

$$\varphi_1(z) = \frac{\kappa_2 + 1}{\kappa_1 + 1}\varphi_2(z) = -\frac{i\mu(b_1 + ib_2)}{\pi(\kappa_1 + 1)}\ln(z - z_0), \quad z \in S_1 \cup S_2; \tag{6}$$

$$\psi_1(z) + \frac{\kappa_2 - \kappa_1}{\kappa_1 + 1}\overline{\varphi_2(z)} + \frac{\kappa_2 - \kappa_1}{\kappa_1 + 1}(z^{1/2} - 2H^{1/2})^2\varphi_2'(z) = \psi_2(z), \quad z \in L. \tag{7}$$

Equation (6) serves as an analytic continuation of the two analytic functions $\varphi_1(z)$ and $\varphi_2(z)$. In writing (7), we have adopted the identity that $\bar{z}^{1/2} = 2H^{1/2} - z^{1/2}$ for $z \in L$. This identity will also be used in the following derivations. It remains to determine the two analytic functions $\psi_1(z)$ and $\psi_2(z)$ through satisfaction of (7). In the ensuing three sections, $\psi_1(z)$ and $\psi_2(z)$ will be derived separately for the three cases in which an edge dislocation is located in the matrix, in the parabolic inhomogeneity and on the interface.

3.2. *An edge dislocation in the matrix.* When the edge dislocation is located in the matrix, it follows from (7) and the identity: $\ln(\bar{z} - \bar{z}_0) = \ln(z^{1/2} - \bar{z}_0^{1/2} - 2H^{1/2}) + \ln(z^{1/2} + \bar{z}_0^{1/2} - 2H^{1/2})$, $z \in L$ that the two analytic functions $\psi_1(z)$ and $\psi_2(z)$ can be determined explicitly as

$$\psi_1(z) = \frac{i\mu(\kappa_1 - \kappa_2)(b_1 - ib_2)}{\pi(\kappa_1 + 1)(\kappa_2 + 1)} \ln[z - (\bar{z}_0^{1/2} + 2H^{1/2})^2]$$

$$+ \frac{i\mu(b_1 - ib_2)}{\pi(\kappa_2 + 1)} \ln(z - z_0) + \frac{i\mu(b_1 + ib_2)}{\pi(\kappa_2 + 1)} \frac{\bar{z}_0}{z - z_0} + \frac{i\mu(\kappa_2 - \kappa_1)(b_1 + ib_2)}{\pi(\kappa_1 + 1)(\kappa_2 + 1)} \frac{(2H^{1/2} - z_0^{1/2})^2}{z - z_0},$$

$$z \in S_1; \quad (8)$$

$$\psi_2(z) = \frac{i\mu(b_1 - ib_2)}{\pi(\kappa_2 + 1)} \ln(z - z_0) + \frac{i\mu(b_1 + ib_2)}{\pi(\kappa_2 + 1)} \frac{\bar{z}_0}{z - z_0} + \frac{i\mu(\kappa_2 - \kappa_1)(b_1 + ib_2)}{\pi(\kappa_1 + 1)(\kappa_2 + 1)} \frac{4H^{1/2}}{z^{1/2} + z_0^{1/2}}$$

$$+ \frac{i\mu(\kappa_2 - \kappa_1)(b_1 - ib_2)}{\pi(\kappa_1 + 1)(\kappa_2 + 1)} \ln(z^{1/2} + \bar{z}_0^{1/2} - 2H^{1/2}) + \frac{i\mu(\kappa_1 - \kappa_2)(b_1 - ib_2)}{\pi(\kappa_1 + 1)(\kappa_2 + 1)} \ln(z^{1/2} + \bar{z}_0^{1/2} + 2H^{1/2}),$$

$$z \in S_2, \quad (9)$$

where the branch cut for $z^{1/2}$ is chosen as the negative x_1-axis. In obtaining (8) and (9), one must ensure that $\psi_1(z)$ defined in the parabolic inhomogeneity is indeed an analytic function of z. The stresses in the composite induced by the edge dislocation in the matrix can be arrived at by substituting (6), (8) and (9) into (1). Using the Peach–Koehler formula [Dundurs 1969], the image force acting on the edge dislocation can be explicitly determined as follows:

$$F_1 = \frac{H^{1/2}\mu(\kappa_2 - \kappa_1)}{2\pi r^{3/2}(\kappa_1 + 1)(\kappa_2 + 1)} \left[(b_2^2 - b_1^2)\cos\frac{3\theta}{2} - 2b_1 b_2 \sin\frac{3\theta}{2} + \frac{2r(b_1^2 + b_2^2)}{r(1 + \cos\theta) - 2H} \cos\frac{\theta}{2} \right],$$

$$F_2 = \frac{H^{1/2}\mu(\kappa_2 - \kappa_1)}{2\pi r^{3/2}(\kappa_1 + 1)(\kappa_2 + 1)} \left[(b_2^2 - b_1^2)\sin\frac{3\theta}{2} + 2b_1 b_2 \cos\frac{3\theta}{2} + \frac{2r(b_1^2 + b_2^2)}{r(1 + \cos\theta) - 2H} \sin\frac{\theta}{2} \right], \quad (10)$$

where F_1 and F_2 are, respectively, the force components along the x_1 and x_2 directions. We see that the image force in (10) varies with the direction of the vector (b_1, b_2).

When the edge dislocation lies on the x_1-axis, Equation (10) becomes

$$F_1 = \frac{H^{1/2}\mu(\kappa_2 - \kappa_1)}{2\pi r^{3/2}(\kappa_1 + 1)(\kappa_2 + 1)} \left[b_2^2 - b_1^2 + \frac{r(b_1^2 + b_2^2)}{r - H} \right], \quad F_2 = \frac{H^{1/2}\mu(\kappa_2 - \kappa_1)b_1 b_2}{\pi r^{3/2}(\kappa_1 + 1)(\kappa_2 + 1)}. \quad (11)$$

When the edge dislocation approaches the vertex of the parabola L, Equation (11) reduces to

$$F_1 = \frac{\mu(\kappa_2 - \kappa_1)(b_1^2 + b_2^2)}{2\pi(\kappa_1 + 1)(\kappa_2 + 1)(r - H)}, \quad F_2 = \frac{\mu(\kappa_2 - \kappa_1)b_1 b_2}{\pi H(\kappa_1 + 1)(\kappa_2 + 1)}, \quad \text{as } r \to H. \quad (12)$$

The expression for F_1 in (12) is simply the classical result for an edge dislocation interacting with a planar bimaterial interface [Dundurs 1969]. On the other hand, when the edge dislocation lying on the x_1-axis is further from the parabola L, Equation (11) reduces to

$$F_1 \cong \frac{H^{1/2}\mu(\kappa_2 - \kappa_1)b_2^2}{\pi r^{3/2}(\kappa_1 + 1)(\kappa_2 + 1)} + O(r^{-\frac{5}{2}}), \quad F_2 = \frac{H^{1/2}\mu(\kappa_2 - \kappa_1)b_1 b_2}{\pi r^{3/2}(\kappa_1 + 1)(\kappa_2 + 1)}, \quad \text{as } r \to \infty, \quad (13)$$

which implies that the far-field asymptotic behavior of F_1 is dominated by the b_2 component of the Burgers vector.

3.3. An edge dislocation in the parabolic inhomogeneity.
When the edge dislocation is located in the parabolic inhomogeneity, it follows from (7) that the two analytic functions $\psi_1(z)$ and $\psi_2(z)$ can be explicitly determined as

$$\psi_1(z) = \frac{i\mu(b_1 - ib_2)}{\pi(\kappa_1 + 1)} \ln(z - z_0) + \frac{i\mu(b_1 + ib_2)}{\pi(\kappa_1 + 1)} \frac{\bar{z}_0}{z - z_0}$$
$$+ \frac{i\mu(\kappa_1 - \kappa_2)(b_1 - ib_2)}{\pi(\kappa_1 + 1)(\kappa_2 + 1)} \{\ln[z - (\bar{z}_0^{1/2} - 2H^{1/2})^2] + \ln[z - (\bar{z}_0^{1/2} + 2H^{1/2})^2]\}, \quad z \in S_1; \quad (14)$$

$$\psi_2(z) = \frac{i\mu(b_1 - ib_2)}{\pi(\kappa_1 + 1)} \ln(z - z_0) + \frac{i\mu(b_1 + ib_2)}{\pi(\kappa_1 + 1)} \frac{\bar{z}_0}{z - z_0} + \frac{i\mu(\kappa_1 - \kappa_2)(b_1 + ib_2)}{\pi(\kappa_1 + 1)(\kappa_2 + 1)} \frac{(z^{1/2} - 2H^{1/2})^2}{z - z_0}$$
$$+ \frac{i\mu(\kappa_1 - \kappa_2)(b_1 - ib_2)}{\pi(\kappa_1 + 1)(\kappa_2 + 1)} [\ln(z^{1/2} - \bar{z}_0^{1/2} + 2H^{1/2}) + \ln(z^{1/2} + \bar{z}_0^{1/2} + 2H^{1/2})], \quad z \in S_2. \quad (15)$$

The stresses in the composite induced by the edge dislocation in the inhomogeneity can be arrived at by substituting (6), (14) and (15) into (1). Using the Peach–Koehler formula, the image force acting on the edge dislocation can be explicitly determined as follows

$$F_1 = \frac{2\mu(\kappa_1 - \kappa_2)(b_1^2 + b_2^2)}{\pi(\kappa_1 + 1)(\kappa_2 + 1)} \frac{H}{r^2 \sin^2\theta + 4Hr\cos\theta - 4H^2},$$
$$F_2 = \frac{\mu(\kappa_1 - \kappa_2)(b_1^2 + b_2^2)}{\pi(\kappa_1 + 1)(\kappa_2 + 1)} \frac{r\sin\theta}{r^2 \sin^2\theta + 4Hr\cos\theta - 4H^2}, \quad (16)$$

which implies that the image force is invariant with the direction of the vector (b_1, b_2).

When the edge dislocation lies on the x_1-axis, (16) becomes

$$F_1 = \frac{\mu(\kappa_2 - \kappa_1)(b_1^2 + b_2^2)}{2\pi(\kappa_1 + 1)(\kappa_2 + 1)(H - x_0)}, \quad F_2 = 0, \quad -\infty < x_0 \le H. \quad (17)$$

Interestingly, Equation (17) is always identical in form to the result for an edge dislocation near a planar interface [Dundurs 1969]. We interpret from (17) that as far as the force on the edge dislocation is concerned, an edge dislocation lying on the axis of symmetry of the parabola L can be treated as equivalent to the same edge dislocation near a planar bimaterial interface at $\{x_1 = H, -\infty < x_2 < +\infty\}$. We illustrate in Figure 2 the variation of F_1 with an edge dislocation on the x_1-axis. It is seen from Figure 2 and from our previous analysis that as the edge dislocation is further away from the vertex of the parabola L, the image force decays faster in the matrix than in the parabolic inhomogeneity, especially when $b_2 = 0$.

3.4. An edge dislocation on the parabolic interface.
When the edge dislocation is located precisely on the parabolic interface with $z_0^{1/2} + \bar{z}_0^{1/2} = 2H^{1/2}$, the two analytic functions $\psi_1(z)$ and $\psi_2(z)$ can be obtained either from (8) and (9) or from (14) and (15) as

$$\psi_1(z) = \frac{i\mu(b_1 - ib_2)}{\pi(\kappa_2 + 1)} \ln(z - z_0) + \frac{i\mu(b_1 + ib_2)}{\pi(\kappa_1 + 1)} \frac{\bar{z}_0}{z - z_0} + \frac{i\mu(\kappa_1 - \kappa_2)(b_1 - ib_2)}{\pi(\kappa_1 + 1)(\kappa_2 + 1)} \ln[z - (\bar{z}_0^{1/2} + 2H^{1/2})^2],$$
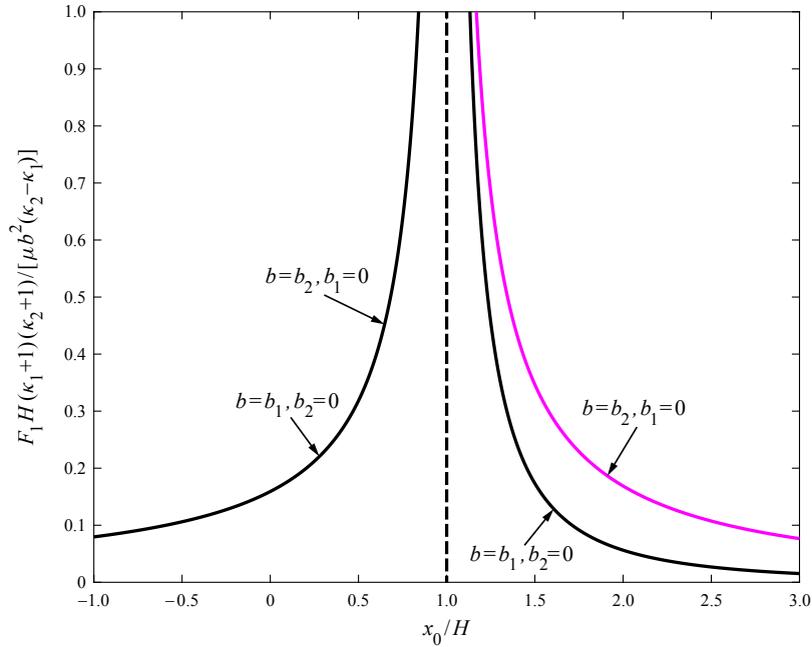$$z \in S_1; \quad (18)$$

Figure 2. Variation of the image force F_1 on an edge dislocation on the x_1-axis in the matrix and in the parabolic inhomogeneity.

$$\psi_2(z) = \frac{i\mu(b_1 - ib_2)}{\pi(\kappa_1 + 1)} \ln(z - z_0) + \frac{i\mu(b_1 + ib_2)}{\pi(\kappa_2 + 1)} \frac{\bar{z}_0}{z - z_0} + \frac{i\mu(\kappa_2 - \kappa_1)(b_1 + ib_2)}{\pi(\kappa_1 + 1)(\kappa_2 + 1)} \frac{4H^{1/2}}{z^{1/2} + z_0^{1/2}}$$
$$+ \frac{i\mu(\kappa_1 - \kappa_2)(b_1 - ib_2)}{\pi(\kappa_1 + 1)(\kappa_2 + 1)} [\ln(z^{1/2} + z_0^{1/2}) + \ln(z^{1/2} + \bar{z}_0^{1/2} + 2H^{1/2})], \quad z \in S_2. \quad (19)$$

The development of the (identical) expressions for the two analytic functions $\psi_1(z)$ and $\psi_2(z)$ in (18) and (19) whether obtained from (8) and (9) (when the edge dislocation is located in the matrix) or from (14) and (15) (when the edge dislocation lies inside the inhomogeneity) not only suggests the rationale for the solutions derived in the following Secs. 4 and 5 but also confirms their correctness. The stresses in the composite induced by the edge dislocation located precisely on the parabolic interface can be obtained by substituting (6), (18) and (19) into (1).

4. An edge dislocation interacting with an elliptical elastic inhomogeneity

As shown in Figure 3, an elliptical elastic inhomogeneity, denoted by S_1, is perfectly bonded to the surrounding matrix, denoted by S_2, through an elliptical interface L described by

$$L : \frac{x_1^2}{a^2} + \frac{x_2^2}{b^2} = 1, \quad (20)$$

with a and b being the semi-major and semi-minor axes of the ellipse L, respectively. In addition, an edge dislocation with Burgers vector (b_1, b_2) is located at $z = z_0 = x_0 + iy_0$ with x_0 and y_0 being the Cartesian coordinates of z_0. As before, subscript 1 and 2 are used to identify the respective quantities
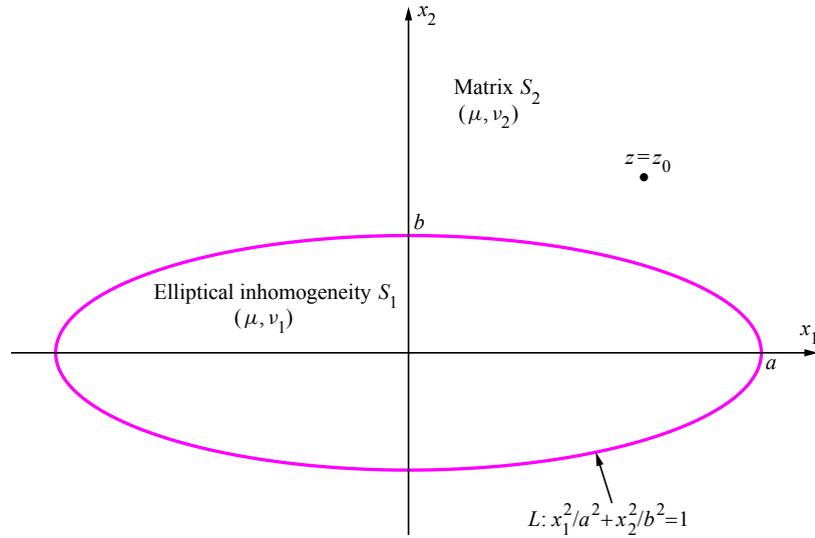
Figure 3. An edge dislocation interacting with an elliptical elastic inhomogeneity. The edge dislocation located at $z = z_0$ can be in the matrix, in the inhomogeneity or just on the elliptical interface.

in S_1 and S_2. The elliptical inhomogeneity and the matrix have the same shear modulus but different Poisson's ratios (i.e., $\mu_1 = \mu_2 = \mu$ and $\nu_1 \neq \nu_2$).

After some algebraic operations, the continuity conditions of tractions and displacements across the perfect elliptical interface L in (5) can be rewritten as

$$\varphi_1(z) = \frac{\kappa_2 + 1}{\kappa_1 + 1}\varphi_2(z) = -\frac{i\mu(b_1 + ib_2)}{\pi(\kappa_1 + 1)}\ln(z - z_0), \quad z \in S_1 \cup S_2; \tag{21}$$

$$\psi_1(z) + \frac{\kappa_2 - \kappa_1}{\kappa_1 + 1}\overline{\varphi_2(z)} + \frac{\kappa_2 - \kappa_1}{\kappa_1 + 1}D(z)\varphi_2'(z) = \psi_2(z), \quad z \in L, \tag{22}$$

where

$$\bar{z} = D(z) = \frac{m + m^{-1}}{2}z + \frac{m - m^{-1}}{2}\sqrt{z^2 - 4mR^2}, \quad z \in L, \tag{23}$$

with

$$R = \frac{a + b}{2}, m = \frac{a - b}{a + b}. \tag{24}$$

When the edge dislocation is located in the matrix, it follows from (22) and the identity: $\ln(\bar{z} - \bar{z}_0) = \ln[R(\xi^{-1} - \bar{\xi}_0)(1 - m\bar{\xi}_0^{-1}\xi)]$, $z \in L$ with

$$\xi = \omega^{-1}(z) = \frac{1}{2R}\left(z + \sqrt{z^2 - 4mR^2}\right) \quad \text{and} \quad \xi_0 = \omega^{-1}(z_0) = \frac{1}{2R}\left(z_0 + \sqrt{z_0^2 - 4mR^2}\right)$$

that the two analytic functions $\psi_1(z)$ and $\psi_2(z)$ can be explicitly determined as

$$\psi_1(z) = \frac{i\mu(\kappa_1 - \kappa_2)(b_1 - ib_2)}{\pi(\kappa_1 + 1)(\kappa_2 + 1)} \ln(z - z_1)$$

$$+ \frac{i\mu(b_1 - ib_2)}{\pi(\kappa_2 + 1)} \ln(z - z_0) + \frac{i\mu(b_1 + ib_2)}{\pi(\kappa_2 + 1)} \frac{\bar{z}_0}{z - z_0} + \frac{i\mu(\kappa_2 - \kappa_1)(b_1 + ib_2)}{\pi(\kappa_1 + 1)(\kappa_2 + 1)} \frac{D(z_0)}{z - z_0}, \quad z \in S_1; \quad (25)$$

$$\psi_2(z) = \frac{i\mu(b_1 - ib_2)}{\pi(\kappa_2 + 1)} \ln(z - z_0) + \frac{i\mu(b_1 + ib_2)}{\pi(\kappa_2 + 1)} \frac{\bar{z}_0}{z - z_0}$$

$$+ \frac{i\mu(\kappa_1 - \kappa_2)(m - m^{-1})(b_1 + ib_2)}{2\pi(\kappa_1 + 1)(\kappa_2 + 1)} \frac{z + z_0}{\sqrt{z^2 - 4mR^2} + \sqrt{z_0^2 - 4mR^2}}$$

$$+ \frac{i\mu(\kappa_2 - \kappa_1)(b_1 - ib_2)}{\pi(\kappa_1 + 1)(\kappa_2 + 1)} \ln\left[1 - \frac{\bar{\xi}_0^{-1}}{\omega^{-1}(z)}\right] + \frac{i\mu(\kappa_1 - \kappa_2)(b_1 - ib_2)}{\pi(\kappa_1 + 1)(\kappa_2 + 1)} \ln\left[1 - \frac{m^2\bar{\xi}_0^{-1}}{\omega^{-1}(z)}\right], \quad z \in S_2, \quad (26)$$

where

$$z_1 = R(m^{-1}\bar{\xi}_0 + m^2\bar{\xi}_0^{-1}). \tag{27}$$

By using the Peach–Koehler formula, the image force acting on the edge dislocation can be finally derived as follows:

$$F_1 - iF_2 = \frac{R^2\mu(\kappa_2 - \kappa_1)(1 - m^2)}{\pi(\kappa_1 + 1)(\kappa_2 + 1)(z_0^2 - 4mR^2)^{3/2}}$$

$$\times \left[b_2^2 - b_1^2 - 2ib_1b_2 + \frac{4(b_1^2 + b_2^2)(z_0^2 - 4mR^2)|z_0 + \sqrt{z_0^2 - 4mR^2}|^2}{(|z_0 + \sqrt{z_0^2 - 4mR^2}|^2 - 4m^2R^2)(|z_0 + \sqrt{z_0^2 - 4mR^2}|^2 - 4R^2)}\right], \quad (28)$$

where F_1 and F_2 are respectively the force components along the x_1 and x_2 directions.

When an edge dislocation lying on the positive x_1-axis approaches the elliptical interface, (28) becomes

$$F_1 = \frac{\mu(\kappa_2 - \kappa_1)(b_1^2 + b_2^2)}{2\pi(\kappa_1 + 1)(\kappa_2 + 1)(x_0 - a)}, \quad F_2 = \frac{2\mu(\kappa_2 - \kappa_1)b_1b_2}{\pi(\kappa_1 + 1)(\kappa_2 + 1)b^2/a}, \quad x_0 \to a. \tag{29}$$

The expression for F_1 in (29) is just the result for an edge dislocation near a planar bimaterial interface [Dundurs 1969], whilst the expression of F_2 in (29) is consistent with that in (12) by considering the fact that b^2/a is the curvature radius of the ellipse at $z = a$ and $2H$ is the curvature radius of the parabola at the vertex.

On the other hand, when the edge dislocation is far from the interface, (28) reduces to

$$F_1 - iF_2 = \frac{R^2\mu(\kappa_2 - \kappa_1)(1 - m^2)}{\pi(\kappa_1 + 1)(\kappa_2 + 1)z_0^3}\left[b_2^2\left(1 + \frac{z_0}{\bar{z}_0}\right) - b_1^2\left(1 - \frac{z_0}{\bar{z}_0}\right) - 2ib_1b_2\right], \quad |z_0| \to \infty. \tag{30}$$

When $m = 0$ for a circular inhomogeneity, (28) simply reduces to the classical result in Equations (7.8) and (7.9) by [Dundurs 1969].

When the edge dislocation is located inside the elliptical inhomogeneity, it follows from (22) that the two analytic functions $\psi_1(z)$ and $\psi_2(z)$ can be explicitly determined as

$$\psi_1(z) = \frac{i\mu(b_1 - ib_2)}{\pi(\kappa_1 + 1)} \ln(z - z_0) + \frac{i\mu(b_1 + ib_2)}{\pi(\kappa_1 + 1)} \frac{\bar{z}_0}{z - z_0} + \frac{i\mu(\kappa_1 - \kappa_2)(b_1 - ib_2)}{\pi(\kappa_1 + 1)(\kappa_2 + 1)} \ln[(z - z_1)(z - z_2)],$$

$$z \in S_1; \quad (31)$$

$$\psi_2(z) = \frac{i\mu(b_1 - ib_2)}{\pi(\kappa_1 + 1)} \ln(z - z_0) + \frac{i\mu(b_1 + ib_2)}{\pi(\kappa_1 + 1)} \frac{\bar{z}_0}{z - z_0} + \frac{i\mu(\kappa_1 - \kappa_2)(b_1 + ib_2)}{\pi(\kappa_1 + 1)(\kappa_2 + 1)} \frac{D(z)}{z - z_0}$$

$$+ \frac{i\mu(\kappa_1 - \kappa_2)(b_1 - ib_2)}{\pi(\kappa_1 + 1)(\kappa_2 + 1)} \left[\ln\left[1 - \frac{m^2 \bar{\xi}_0^{-1}}{\omega^{-1}(z)} \right] + \ln[\omega^{-1}(z) - m\bar{\xi}_0] \right], \quad z \in S_2, \quad (32)$$

where

$$\xi = \omega^{-1}(z) = \frac{1}{2R}\left(z + \sqrt{z^2 - 4mR^2}\right), \quad z_1 = R(m^{-1}\bar{\xi}_0 + m^2\bar{\xi}_0^{-1}),$$

$$\xi_0 = \omega^{-1}(z_0) = \frac{1}{2R}\left(z_0 + \sqrt{z_0^2 - 4mR^2}\right), \quad z_2 = R(m\bar{\xi}_0 + \bar{\xi}_0^{-1}). \tag{33}$$

By using the Peach–Koehler formula, the image force acting on the edge dislocation can be finally derived as follows

$$F_1 - iF_2 = \frac{\mu(\kappa_1 - \kappa_2)(b_1^2 + b_2^2)}{\pi(\kappa_1 + 1)(\kappa_2 + 1)} \left(\frac{1}{z_0 - z_1} + \frac{1}{z_0 - z_2} \right), \tag{34}$$

which implies that the image force is invariant with the direction of the vector (b_1, b_2). It will be seen in the next section that the invariance of the image force with the direction of the Burger vector is invalid for an edge dislocation inside an elastic inhomogeneity of *nonelliptical shape* having the same shear modulus as that of the matrix.

When the edge dislocation lies on the x_1-axis, (34) becomes

$$F_1 = \frac{\mu(\kappa_2 - \kappa_1)(b_1^2 + b_2^2)}{\pi(\kappa_1 + 1)(\kappa_2 + 1)} \frac{x_0}{a^2 - x_0^2}, \quad F_2 = 0, \tag{35}$$

which is identical to that for an edge dislocation inside a circular elastic inhomogeneity of radius a [Dundurs 1969]. Equation (35) implies that the semi-minor axis b exerts no influence on the image force on an edge dislocation lying on the x_1-axis inside the elliptical inhomogeneity.
When the edge dislocation lies on the x_2-axis, (34) becomes

$$F_2 = \frac{\mu(\kappa_2 - \kappa_1)(b_1^2 + b_2^2)}{\pi(\kappa_1 + 1)(\kappa_2 + 1)} \frac{y_0}{b^2 - y_0^2}, \quad F_1 = 0, \tag{36}$$

which is identical to that for an edge dislocation inside a circular elastic inhomogeneity of radius b [Dundurs 1969]. Equation (36) implies that the semi-major axis a exerts no influence on the image force on an edge dislocation lying on the x_2-axis inside the elliptical inhomogeneity.
Through a limiting process, the two analytic functions $\psi_1(z)$ and $\psi_2(z)$ can be obtained for the case when the edge dislocation just lies on the elliptical interface. The specific expressions are suppressed here.

5. An edge dislocation inside an elastic inhomogeneity of arbitrary shape

In this section, we consider an edge dislocation with Burgers vector (b_1, b_2) located at $z = z_0$ inside an elastic inhomogeneity of arbitrary shape (denoted as S_1) perfectly bonded to the surrounding infinite matrix (denoted as S_2) through a sharp interface L. Here, we use the term "sharp interface" to mean an interface with vanishing thickness between two dissimilar adjacent phases. As before, subscript 1 and 2 are used to identify the respective quantities in S_1 and S_2. The elastic inhomogeneity and the matrix have the same shear modulus but different Poisson's ratios.

We consider the following conformal mapping function [England 1971]:

$$z = \omega(\xi) = R\left(\xi + \sum_{n=1}^{N} a_n \xi^{-n}\right), \quad \xi = \omega^{-1}(z), \quad |\xi| \geq 1, \tag{37}$$

where R is a real scaling constant, and a_n, $n = 1, 2, \ldots, N$ are N complex constants.

By using the mapping function in (37), the exterior of the inhomogeneity is mapped onto the exterior of the unit circle in the ξ-plane.

On the interface L, we have

$$\bar{z} - \bar{z}_0 = R\xi^{-1}\left(\sum_{n=1}^{N} \bar{a}_n \xi^{n+1} - \bar{z}_0 R^{-1} \xi + 1\right) = R\bar{a}_N \xi^{-1} \prod_{n=1}^{N+1} (\xi - \xi_n), \quad z \in L, \tag{38}$$

where ξ_n, $n = 1, 2, \ldots, N+1$, all of which are located outside the unit circle, are the $N+1$ roots of the following $(N+1)$-order algebraic equation in ξ

$$\sum_{n=1}^{N} \bar{a}_n \xi^{n+1} - \bar{z}_0 R^{-1} \xi + 1 = 0. \tag{39}$$

Furthermore, the following relationship is also valid on the interface L

$$\frac{\bar{z}}{z - z_0} = G(z), z \in L, \tag{40}$$

where $G(z)$ is analytic in the exterior of the inhomogeneity except infinity where it has a pole of finite degree determined by its asymptotic behavior

$$G(z) \cong Q(z) + O(1), \quad |z| \to \infty, \tag{41}$$

where $Q(z)$ is a polynomial in z of $(N-1)$-degree. Apparently, the polynomial $Q(z)$ is non-constant for a nonelliptical inhomogeneity with $N \geq 2$ and is constant for an elliptical inhomogeneity with $N = 1$.

The analytic function $\phi_1(z)$ defined in the inhomogeneity is still given by (21). Consequently, the analytic function $\psi_1(z)$ defined in the inhomogeneity can be finally determined as

$$\begin{aligned}
\psi_1(z) = {} & \frac{i\mu(b_1 - ib_2)}{\pi(\kappa_1 + 1)} \ln(z - z_0) + \frac{i\mu(b_1 + ib_2)}{\pi(\kappa_1 + 1)} \frac{\bar{z}_0}{z - z_0} \\
& + \frac{i\mu(\kappa_1 - \kappa_2)(b_1 - ib_2)}{\pi(\kappa_1 + 1)(\kappa_2 + 1)} \sum_{n=1}^{N+1} \ln(z - z_n) + \frac{i\mu(\kappa_2 - \kappa_1)(b_1 + ib_2)}{\pi(\kappa_1 + 1)(\kappa_2 + 1)} Q(z), \quad z \in S_1,
\end{aligned} \tag{42}$$

where

$$z_n = \omega(\xi_n), n = 1, 2, \ldots, N+1. \tag{43}$$

By using the Peach–Koehler formula, the image force acting on the edge dislocation is

$$F_1 - iF_2 = \frac{\mu(\kappa_1 - \kappa_2)}{\pi(\kappa_1 + 1)(\kappa_2 + 1)} \left[(b_1^2 + b_2^2) \sum_{n=1}^{N+1} \frac{1}{z_0 - z_n} - (b_1^2 - b_2^2 + 2ib_1b_2) Q'(z_0) \right], \tag{44}$$

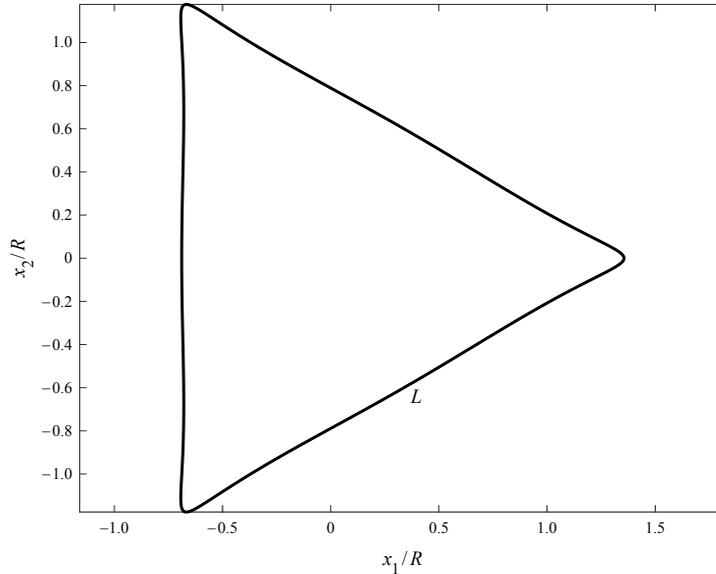so that the image force varies with the direction of the vector (b_1, b_2) for an inhomogeneity of nonellip-

Figure 4. A rounded triangular interface L described by Equation (45).

tical shape. The image force is known once z_n, $n = 1, 2, \ldots, N + 1$ and $Q'(z_0)$ have been determined.

For example, we consider a rounded triangular interface in Figure 4 described by

$$z = \omega(\xi) = R\left(\xi + \frac{1}{3\xi^2} + \frac{1}{45\xi^5}\right), \quad |\xi| = 1. \tag{45}$$

In this example, $N = 5$. The polynomial $Q(z)$ is explicitly determined by

$$Q(z) = \frac{z^4 + z_0 z^3 + z_0^2 z^2}{45R^4} + z\left(\frac{z_0^3}{45R^4} + \frac{8}{27R}\right). \tag{46}$$

Thus, the term $Q'(z_0)$ can be easily determined by

$$Q'(z_0) = \frac{2z_0^3}{9R^4} + \frac{8}{27R}. \tag{47}$$

The image force on an edge dislocation on the x_1-axis inside the rounded triangular inhomogeneity is illustrated in Figure 5. It is seen from Figure 5 that: $z_0 = -0.1647R$ is an equilibrium position for an edge dislocation with $b_2 = 0$; whilst $z_0 = 0.2240R$ is an equilibrium position for an edge dislocation with $b_1 = 0$. The variance of the image force with the direction of the Burgers vector is also clearly reflected in Figure 5.

6. An edge dislocation outside an elastic inhomogeneity of arbitrary shape

We now consider an edge dislocation with Burgers vector (b_1, b_2) located at $z = z_0$ in an infinite matrix (denoted as S_2) perfectly bonded to an elastic inhomogeneity of arbitrary shape (denoted as S_1) through a sharp interface L. As before, subscript 1 and 2 are used to identify the respective quantities in S_1 and S_2. The elastic inhomogeneity and the matrix have the same shear modulus but different Poisson's ratios.
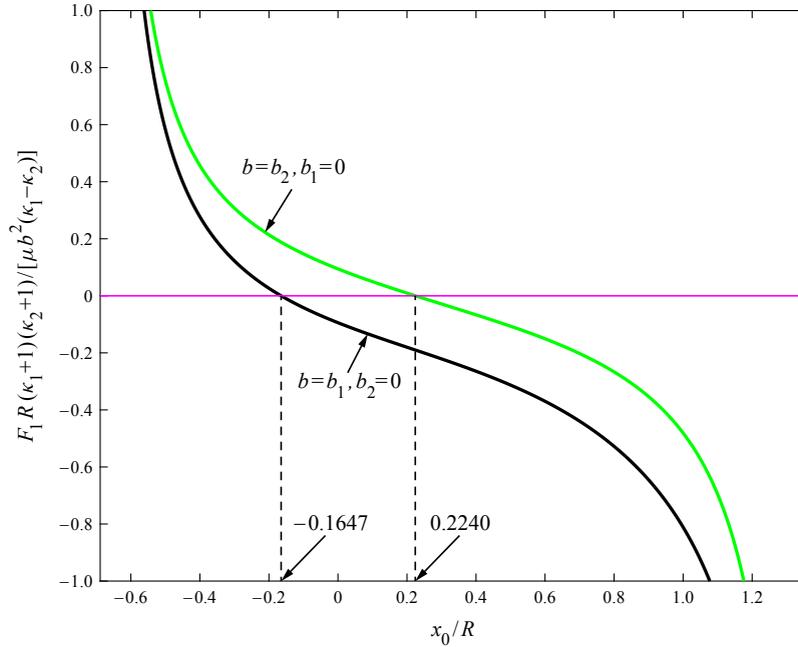
Figure 5. The image force on an edge dislocation on the x_1-axis inside the rounded triangular inhomogeneity. $F_2 \equiv 0$.

We consider the conformal mapping function [Muskhelishvili 1953; Jarczyk and Mityushev 2012]

$$z = \omega(\xi) = R \sum_{n=1}^{M} c_n \xi^n, \xi = \omega^{-1}(z), \quad |\xi| \le 1, \tag{48}$$

where R is a real scaling constant, and $c_n, n = 1, 2, \ldots, M$ are M complex constants. Without losing generality, one can set $c_1 = 1$.

By using the mapping function in (48), the interior of the inhomogeneity is mapped onto the interior of the unit circle in the ξ-plane.

On the interface L, the following relationship is valid

$$\bar{z} - \bar{z}_0 = -\xi^{-M} \left(\bar{z}_0 \xi^M - R \sum_{n=1}^{M} \bar{c}_n \xi^{M-n} \right) = -\bar{z}_0 \xi^{-M} \prod_{n=1}^{M} (\xi - \xi_n), \quad z \in L, \tag{49}$$

where $\xi_n, n = 1, 2, \ldots, M$, all of which are located inside the unit circle, are the M roots of the following M-order algebraic equation in ξ

$$\bar{z}_0 \xi^M - R \sum_{n=1}^{M} \bar{c}_n \xi^{M-n} = 0. \tag{50}$$

The following relationship is also valid on the interface L:

$$\frac{\bar{z}}{z - z_0} = H(z), \ z \in L, \tag{51}$$

where $H(z)$ is analytic in the interior of the inhomogeneity except the point at $z = 0$ where it has a pole of finite degree determined by its asymptotic behavior

$$H(z) \cong P(z) + O(1), \quad z \to 0, \tag{52}$$

where $P(z)$ is a polynomial in z^{-1} of degree M.

The analytic function $\phi_2(z)$ defined in the matrix is still given by (21). Consequently, the analytic function $\psi_2(z)$ defined in the matrix can be finally determined as

$$\psi_2(z) = \frac{i\mu(b_1 - ib_2)}{\pi(\kappa_2 + 1)} \ln(z - z_0) + \frac{i\mu(b_1 + ib_2)}{\pi(\kappa_2 + 1)} \frac{\bar{z}_0}{z - z_0}$$
$$+ \frac{i\mu(\kappa_2 - \kappa_1)(b_1 - ib_2)}{\pi(\kappa_1 + 1)(\kappa_2 + 1)} \sum_{n=1}^{M} \ln \frac{z - z_n}{z} + \frac{i\mu(\kappa_1 - \kappa_2)(b_1 + ib_2)}{\pi(\kappa_1 + 1)(\kappa_2 + 1)} P(z), \quad z \in S_2, \tag{53}$$

where

$$z_n = \omega(\xi_n), \quad n = 1, 2, \ldots, M. \tag{54}$$

By using the Peach–Koehler formula, the image force acting on the edge dislocation is

$$F_1 - iF_2 = \frac{\mu(\kappa_2 - \kappa_1)}{\pi(\kappa_1 + 1)(\kappa_2 + 1)} \left[(b_1^2 + b_2^2) \sum_{n=1}^{M} \frac{z_n}{z_0(z_0 - z_n)} - (b_1^2 - b_2^2 + 2ib_1b_2) P'(z_0) \right], \tag{55}$$

which also implies that the image force varies with the direction of the vector (b_1, b_2) when $P'(z_0) \neq 0$. When $M = 1$ for a circular inhomogeneity, we have $z_1 = R^2/\bar{z}_0$ and $P'(z_0) = R^2/z_0^3$. In this special case, (55) simply recovers the classical result in Equations (7.8) and (7.9) by [Dundurs 1969].

For example, as illustrated in Figure 6, we consider an interface described by

$$z = \omega(\xi) = R(\xi + c\xi^2), \quad -\tfrac{1}{2} \le c \le \tfrac{1}{2}, \quad |\xi| = 1. \tag{56}$$

In this example, $M = 2$. The two roots of Equation (50) can be explicitly given by

$$\xi_{1,2} = \frac{R \pm \sqrt{R^2 + 4Rc\bar{z}_0}}{2\bar{z}_0}, \quad |\xi_{1,2}| < 1, \tag{57}$$

and thus,

$$z_1 = \frac{cR^3 + R^2\bar{z}_0(2c^2 + 1) + R(\bar{z}_0 + Rc)\sqrt{R^2 + 4Rc\bar{z}_0}}{2\bar{z}_0^2},$$
$$z_2 = \frac{cR^3 + R^2\bar{z}_0(2c^2 + 1) - R(\bar{z}_0 + Rc)\sqrt{R^2 + 4Rc\bar{z}_0}}{2\bar{z}_0^2}. \tag{58}$$

In addition, the polynomial $P(z)$ is determined by

$$P(z) = -\frac{R^2(1 + 2c^2 + Rz_0^{-1}c)}{z_0 z} - \frac{R^3 c}{z_0 z^2}. \tag{59}$$
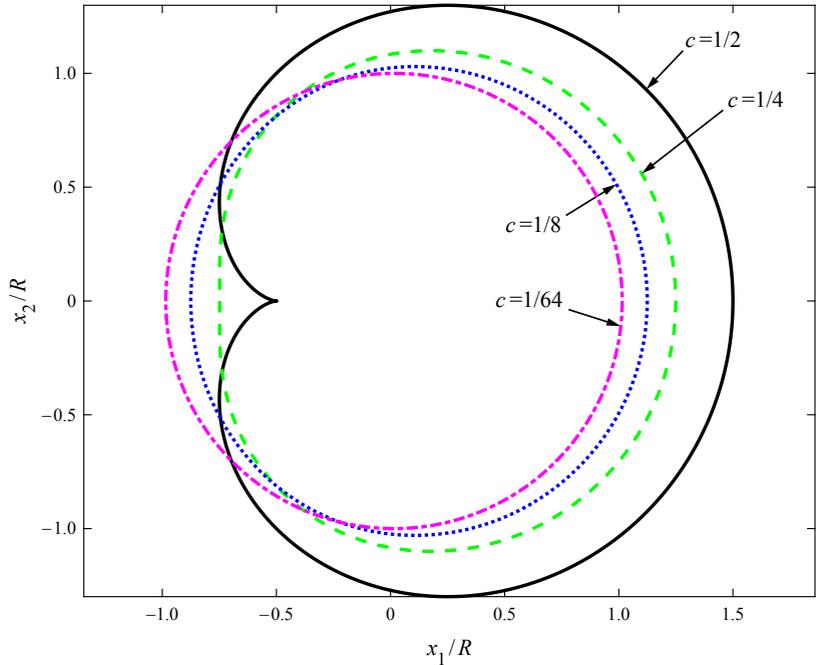
Figure 6. Shapes of the interface described by (56) for different values of c.

Thus, the term $P'(z_0)$ can be easily determined by

$$P'(z_0) = \frac{R^2 z_0 (1 + 2c^2) + 3R^3 c}{z_0^4}.$$ (60)

Consequently, the image force can be given explicitly by

$$
\begin{aligned}
F_1 - \mathrm{i} F_2 &= \frac{\mu(\kappa_2 - \kappa_1)}{\pi(\kappa_1 + 1)(\kappa_2 + 1)} \\
&\times \left(\frac{2R^2 z_0^{-1}(b_1^2 + b_2^2)[[cR + \bar{z}_0(2c^2 + 1)][2z_0\bar{z}_0^2 - cR^3 - R^2\bar{z}_0(2c^2 + 1)] + R(\bar{z}_0 + Rc)^2(R + 4c\bar{z}_0)]}{[2z_0\bar{z}_0^2 - cR^3 - R^2\bar{z}_0(2c^2 + 1)]^2 - R^3(\bar{z}_0 + Rc)^2(R + 4c\bar{z}_0)} \right. \\
&\qquad\qquad\qquad\qquad \left. - R^2 z_0^{-4}(b_1^2 - b_2^2 + 2\mathrm{i}b_1 b_2)[z_0(1 + 2c^2) + 3Rc] \right)
\end{aligned}
$$ (61)

In particular, if we set $c = 1/2$ and $z_0 = R(2 + \mathrm{i})$, the image force on the edge dislocation can be determined from (61) as follows:

$$
\begin{aligned}
F_1 &= \frac{\mu(\kappa_2 - \kappa_1)(0.2704 b_1^2 + 0.2848 b_2^2 - 0.3792 b_1 b_2)}{\pi R(\kappa_1 + 1)(\kappa_2 + 1)}, \\
F_2 &= \frac{\mu(\kappa_2 - \kappa_1)(-0.0345 b_1^2 + 0.3447 b_2^2 + 0.0144 b_1 b_2)}{\pi R(\kappa_1 + 1)(\kappa_2 + 1)}.
\end{aligned}
$$ (62)

It can be seen from (60) and (61) that when the dislocation is located at the following particular point

$$z_0 = -\frac{3Rc}{1+2c^2}, \quad 0.2779 \le |c| \le 0.5, \tag{63}$$

the image force remains invariant with the direction of the Burgers vector and is given by

$$F_1 = \frac{\mu(\kappa_2 - \kappa_1)(b_1^2 + b_2^2)(2c^2 + 1)^5}{6\pi R(\kappa_1 + 1)(\kappa_2 + 1)c(c^2 - 1)(4c^6 + 12c^4 + 12c^2 - 1)}, \quad F_2 = 0. \tag{64}$$

The component F_1 in (64) becomes infinite as $c \to \pm 0.2779$ since now the edge dislocation just approaches the interface L in view of (56) and (63).

7. Conclusions

We have obtained simple and closed-form Green's function solutions for an edge dislocation interacting with a parabolic or elliptical elastic inhomogeneity under the assumption that the inhomogeneity and the matrix have equal shear moduli. For the interaction between an edge dislocation and a parabolic elastic inhomogeneity, the two analytic functions $\psi_1(z)$ and $\psi_2(z)$ are obtained in (8) and (9) for an edge dislocation in the matrix, in (14) and (15) for an edge dislocation in the parabolic inhomogeneity and in (18) and (19) for an edge dislocation located on the parabolic interface; the image force is given by (10) when the dislocation lies in the matrix and by (16) when the dislocation lies in the parabolic inhomogeneity. For the interaction between an edge dislocation and an elliptical elastic inhomogeneity, the two analytic functions $\psi_1(z)$ and $\psi_2(z)$ are obtained in (25) and (26) for an edge dislocation in the matrix, in (31) and (32) for an edge dislocation in the elliptical inhomogeneity; the image force is given by (28) when the dislocation lies in the matrix and by (34) when the dislocation lies in the elliptical inhomogeneity.

We have also obtained closed-form expressions in (44) and (55) for the image force on an edge dislocation in the interior and exterior of an elastic inhomogeneity of arbitrary shape. It is stressed that the mapping function in (37) that maps the exterior of an inhomogeneity onto the exterior of the unit circle in the image plane is distinct from the one in (48) that maps the interior of an inhomogeneity onto the interior of a unit circle in the image plane.

Acknowledgements

References

[Argatov et al. 2012] I. I. Argatov, R. Guinovart-Díaz, and F. J. Sabina, "On local indentation and impact compliance of isotropic auxetic materials from the continuum mechanics viewpoint", *Int. J. Eng. Science* **54** (2012), 42–57.

[Chen 1996] D. H. Chen, "Green's functions for a point force and dislocation outside an elliptic inclusion in plane elasticity", *Z. angew. Math. Phys.* **47** (1996), 894–905.

[Dundurs 1969] J. Dundurs, "Elastic interaction of dislocations with inhomogeneities", pp. 70–115 in *Mathematical theory of dislocations*, edited by T. Mura, American Society of Mechanical Engineers, New York, 1969.

[England 1971] A. H. England, *Complex variable method in elasticity*, John Wiley and Sons, New York, 1971.

[Gong and Meguid 1994] S. X. Gong and S. A. Meguid, "A screw dislocation interacting with an elastic elliptical inhomogeneity", *Int. J. Eng. Sci.* **32** (1994), 1221–1228.

[Jarczyk and Mityushev 2012] P. Jarczyk and V. Mityushev, "Neutral coated inclusions of finite conductivity", *Proc. R. Soc. A* **468**:2140 (2012), 954–970.

[Lakes 1987] R. S. Lakes, "Foam structures with a negative Poisson's ratio", *Science* **235**:4792 (1987), 1038–1040.

[Muskhelishvili 1953] N. I. Muskhelishvili, *Some basic problems of the mathematical theory of elasticity*, Noordhoff, Groningen, 1953.

[Qaissaunee and Santare 1995] M. T. Qaissaunee and M. H. Santare, "Edge dislocation interacting with an elliptical inclusion surrounded by an interfacial zone", *Quart. J. Mech. Appl. Math.* **48**:3 (1995), 465–482.

[Shi and Li 2006] J. Shi and Z. Li, "An approximate solution of the interaction between an edge dislocation and an inclusion of arbitrary shape", *Mech. Res. Commun.* **33** (2006), 804–810.

[Stagni 1982] L. Stagni, "On the elastic field perturbation by inhomogeneities in plane elasticity", *Z. Angew. Math. Phys.* **33** (1982), 315–325.

[Stagni 1993] L. Stagni, "Edge dislocation near an elliptic inhomogeneity with either an adhering or a slipping interface: A comparative study", *Phil. Mag.* **68** (1993), 49–57.

[Stagni 1999] L. Stagni, "The effect of the interface on the interaction of an interior edge dislocation with an elliptical inhomogeneity", *Z. angew. Math. Phys.* **50** (1999), 327–337.

[Stagni and Lizzio 1983] L. Stagni and R. Lizzio, "Shape effects in the interaction between an edge dislocation and elliptical inhomogeneity", *J. Appl. Phys. A* **30** (1983), 217–221.

[Suo 1989] Z. G. Suo, "Singularities interacting with interfaces and cracks", *Int. J. Solids Struct.* **25** (1989), 1133–1142.

[Suo 1990] Z. G. Suo, "Singularities, interfaces and cracks in dissimilar anisotropic media", *Proc. Roy. Soc. London Ser. A* **427**:1873 (1990), 331–358.

[Ting 1996] T. C. T. Ting, *Anisotropic elasticity: theory and applications*, Oxford University Press, New York, 1996.

[Tsuchida et al. 1991] E. Tsuchida, M. Ohno, and D. A. Kouris, "Effects of an inhomogeneous elliptic insert on the elastic field of an edge dislocation", *Solids Mater.* **53** (1991), 285–291.

[Wang 2015] X. Wang, "Eshelby's inclusion and dislocation problems for an isotropic circular domain bonded to an anisotropic medium", *Acta Mech.* **226** (2015), 103–121.

[Wang and Sudak 2006] X. Wang and L. J. Sudak, "Interaction of a screw dislocation with an arbitrary shaped elastic inhomogeneity", *ASME J. Appl. Mech.* **73** (2006), 206–211.

[Warren 1983] W. E. Warren, "The edge dislocation inside an elliptical inclusion", *Mech. Mater.* **2**:4 (1983), 319–330.

[Yen et al. 1995] W. J. Yen, C. Hwu, and Y. K. Liang, "Dislocation inside, outside, or on the interface of an anisotropic elliptical inclusion", *ASME J. Appl. Mech.* **62** (1995), 306–311.

XU WANG: xuwang@ecust.edu.cn
School of Mechanical and Power Engineering, East China University of Science and Technology, 130 Meilong Road, Shanghai, 200237, China

PETER SCHIAVONE: p.schiavone@ualberta.ca
Department of Mechanical Engineering, University of Alberta, 10-203 Donadeo Innovation Center for Engineering, Edmonton AB 6G 1H9, Canada

JOURNAL OF MECHANICS OF MATERIALS AND STRUCTURES

msp.org/jomms

Founded by Charles R. Steele and Marie-Louise Steele

Cover photo: Mando Gomez, www.mandolux.com